Watts/De Pont (Eds.)
Progress in Protein-Lipid Interactions 2

CHAPTER 3

Multinuclear NMR studies of bacteriorhodopsin

JOHN L. BOWERS, REBECCA L. SMITH, CHRIS CORETSOPOULOS, A.C. KUNWAR, MAX KENIRY, XI SHAN, H.S. GUTOWSKY and ERIC OLDFIELD

School of Chemical Sciences, University of Illinois at Urbana-Champaign, 505 South Mathews Avenue, Urbana, IL 61801, U.S.A.

I. Introduction

In this chapter we review our current progress in the study of membrane structure using NMR methods. We focus on the determination of the static and dynamic structure of a membrane protein, bacteriorhodopsin (bR) from the purple membrane of *Halobacterium halobium*, by means of ^{2}H-, ^{13}C-, ^{15}N- and ^{19}F-NMR spectroscopy.

Many physical techniques have been used to characterize the static and dynamic structures of proteins, and in recent years proton NMR has become one of the most powerful methods for determination of the structures of proteins in solution (Wagner and Wüthrich, 1982). Unfortunately, however, such ^{1}H-NMR techniques have only limited applicability to the study of proteins (and lipids) in membranes, because the orientational order in the anisotropic environment of the biomembrane is nonzero. This results in broad, featureless lines, because of the extensive network of dipolar-couplings between protons. Although such interactions can be partially removed by special pulse techniques, the residual linewidths are still too broad to permit high-resolution ^{1}H-NMR of solids as complex as membranes. We thus have to resort to other approaches, and here we discuss the utility of ^{2}H-, ^{13}C-, ^{15}N- and ^{19}F-NMR methods.

Abbreviations: bR, bacteriorhodopsin; CSA, chemical shift anisotropy; CP-MASS, cross-polarization magic angle sample spinning; SDS, sodium dodecylsulfate; TMS, tetramethylsilane.

The immediate advantage of each of these techniques is that isotopic enrichment has to be used, for reasons of sensitivity, which means inter alia that partial spectral assignments are immediately available. The ^{2}H-NMR method was first introduced into the membrane arena over a decade ago (Oldfield et al., 1971; Oldfield and Chapman, 1972) for investigating lipid structure, and in the intervening years much useful information on lipid static and dynamic structure has been obtained by numerous workers (see Seelig, 1977; Smith and Oldfield, 1984, for reviews). More recently, we have used the ^{2}H-NMR method to begin to probe protein structure in biomembranes (Kinsey et al., 1981), and as discussed in this publication, we are now supplementing the ^{2}H-NMR method with ^{13}C-, ^{15}N- and ^{19}F-NMR, to gain further insights into the details of membrane organization.

The purple membrane of *H. halobium*, although atypical of most biological membranes, has several features that are desirable for any physicochemical studies of amino acid dynamics in a membrane protein. First, the purple membrane contains only one type of protein, bacteriorhodopsin, whose structure (Henderson and Unwin, 1975) and amino acid sequence (Ovchinnikov et al., 1978; Khorana et al., 1979) have been characterized. Second, it is the first membrane protein in which the positions of the structural elements, such as α-helices and loops, have been reasonably well established with respect to the amino acid sequence (Ovchinnikov et al., 1979; Engelman and Zaccai, 1980; Ovchinnikov, 1982; Engelman et al., 1982; Agard and Stroud, 1982) and with respect to the surrounding aqueous evironment. Third, *H. halobium* biosynthetically incorporates many specifically labeled amino acids into bR with minimal breakdown or scrambling (Keniry et al., 1984a,b). Fourth, bR is a relatively low molecular weight (~26 000) protein, which means that it is possible to resolve, in suitable instances, individual atomic sites by NMR. And finally, it can be obtained in > 100 mg quantities, even by physical chemists.

The results of our studies to date, as discussed in detail in the following sections, indicate that there are two types of amino acid residues in bR. The first type are characterized as rigid, giving a solid-like powder pattern in ^{2}H-, ^{13}C- and ^{15}N-NMR experiments, while the second category are mobile, and give rise to high-resolution, liquid-like spectra. These results have been used to test the various folding patterns suggested for bR, and it appears that: (1) a membrane surface in bR (±1 residue) may be defined by NMR; (2) all amino acid residues inside the surface are essentially crystalline; (3) all amino acid residues outside the surface are highly mobile on the NMR time scale (~10^{-5} s); (4) NMR data may be used to help evaluate the various structural models; (5) aggregation causes a rigidification of the surface; (6) dehydration causes a rigidification of the bilayer interior.

The picture of surface dynamics obtained from our studies on intact bR is supported by NMR studies of bR that has been either cleaved by trypsin, or crosslinked by carbodiimides.

II. ^{2}H-, ^{13}C-, ^{15}N- and ^{19}F-NMR studies of bacteriorhodopsin

We have obtained ^{2}H-NMR spectra of 12 different amino acid-labeled bR samples, and representative examples are shown in Fig. 1 (Keniry et al., 1984b). Each spectrum is composed of two different types of resonance: a broad powder pattern, and a sharp central component. The broad powder pattern arises from

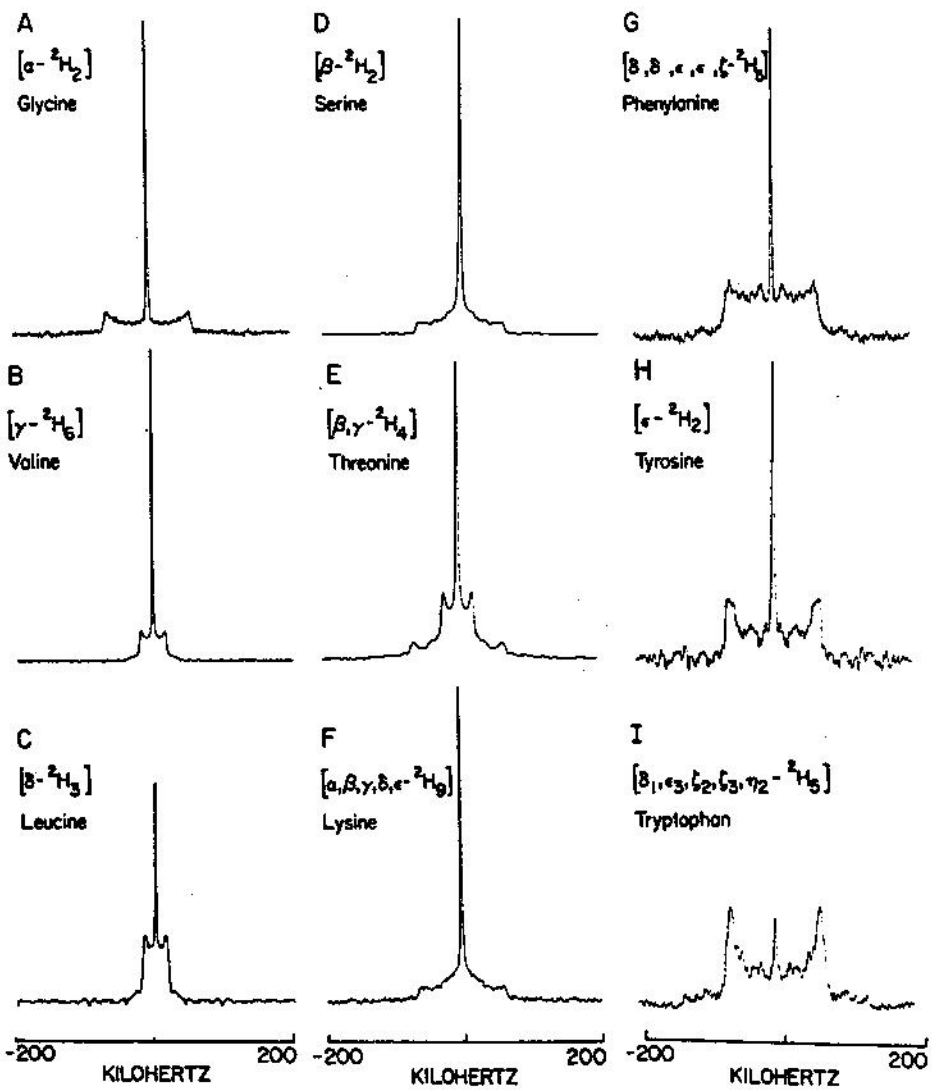

Fig. 1. Deuterium NMR spectra of specifically labeled bRs, at 55.3 MHz (corresponding to a magnetic field strength of 8.45 Tesla) and 4°C.

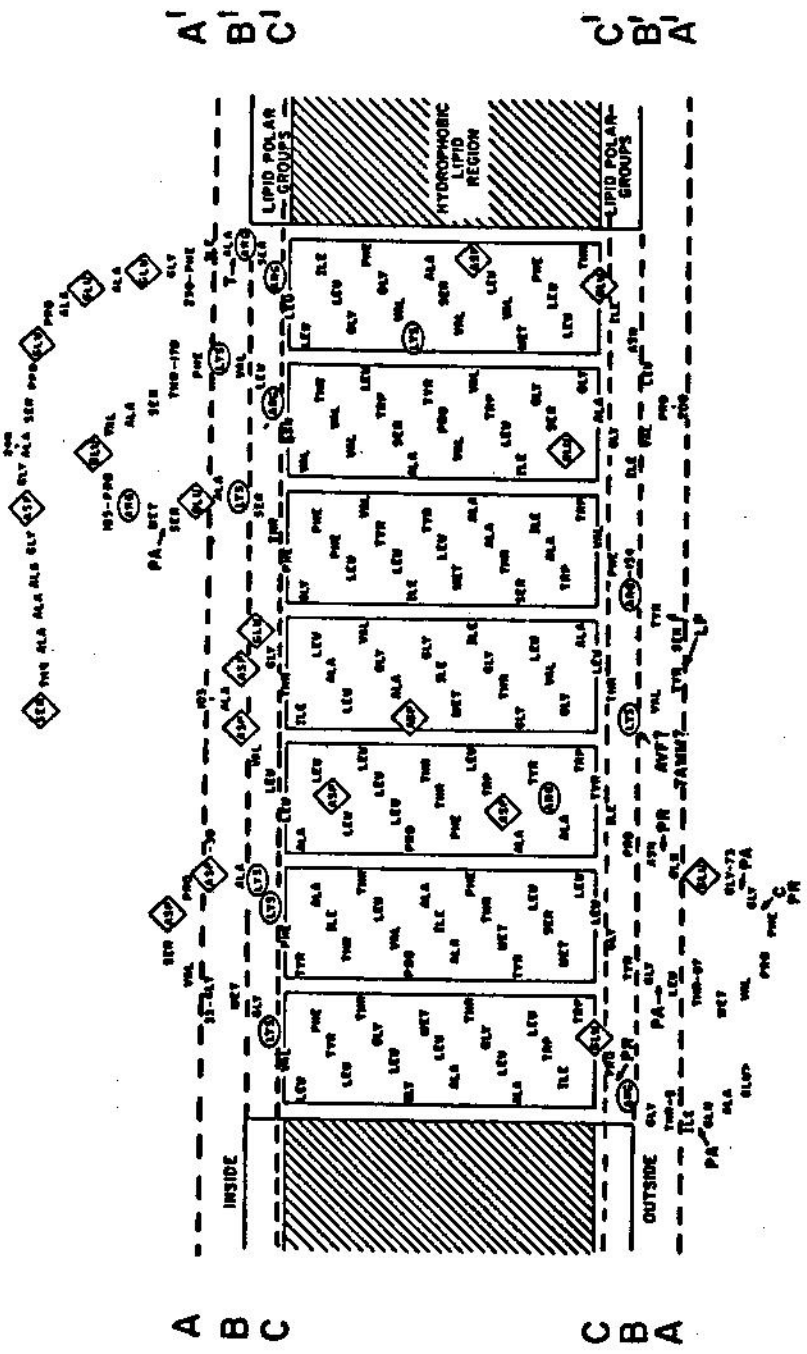
A' B' C'
C' B' A'
LIPID POLAR GROUPS
HYDROPHOBIC LIPID REGION
LIPID POLAR GROUPS
INSIDE
OUTSIDE
A B C
C B A

amino acids which are rigid on the timescale of the ^{2}H-NMR experiment, and the spectral lineshapes and breadths are essentially indistinguishable from those observed with crystalline amino acids (Keniry et al., 1984a). The central component is not seen in ^{2}H-NMR spectra of the free amino acids, and must arise from deuterons in molecules undergoing fast reorientation on the ^{2}H-NMR timescale ($\tau_R \ll 10^{-5}$ s). There are four likely origins of the central components. First, they could arise from residual HO^{2}H (the natural abundance of ^{2}H is 0.016%). Second, they could arise from isotropically tumbling membrane fragments. Third, they could originate from highly mobile surface residues. Fourth, they could be artifacts induced by the quadrupole-echo pulse sequence.

In order to rule out residual HO^{2}H as the source of the central component, its intensity (obtained via computer simulation) was measured as a function of the extent of HO^{2}H exchange, using deuterium-depleted water. Samples were initially exchanged in deuterium-depleted water, then centrifuged for 14 h at 130 000 × *g*, followed by resuspension (in deuterium-depleted water). After the first exchange, the absolute intensity of the central component (for any given labeled bR sample) did not decrease further with additional exchanges. In addition, samples which were depleted of HO^{2}H by lyophilization from ^{2}H-depleted water, followed by resuspension, behaved in a similar manner. Finally, as an additional check, the ^{2}H-NMR spectrum of an *unlabeled* bR sample in ^{2}H-depleted water showed only a very small signal, while in natural ^{2}H-abundance H_2O, the central component was quite intense. These results rule out a significant contribution to the central, isotropic component from natural abundance ^{2}H in H_2O.

The central component could also, at least in principle, arise from membrane fragments undergoing fast, isotropic tumbling (as in the case of sonicated lipid vesicles). If this were the case, the percent central component should be the same for each labeled sample. In sharp contrast to this, the results of Fig. 1 indicate that the percent isotropic component varies widely from amino acid to amino acid. For example, for [$^2H_5$]tryptophan, Fig. 1I, the intensity of the central component is very small, while for [β-$^2H_2$]serine, Fig. 1D, it is very large.

To interpret these results we postulate the idea that *surface residues in native bR are mobile*. To test the idea, we have examined a series of plausible surfaces based on the work of Engelman, Ovchinnikov, Khorana, Stroud and their associates. Residues above the surface, 'surface residues', are assumed to be in an essentially non-structured region, are capable of fast, large angle reorientation, and give rise to the narrow, central component. Residues in the interior of the purple membrane are assumed to be relatively rigid, and give rise to the broad, quadrupolar powder patterns seen in Fig. 1.

Fig. 2. Proposed model of secondary structure of bacteriorhodopsin (Engelman et al., 1982), showing various definitions of the membrane surface(s).

We show in Fig. 2 one typical folding pattern (Engelman et al., 1982) with arbitrary surface lines designated as A-A', B-B', and C-C'. When we analyze the results of Fig. 1 in terms of the model shown in Fig. 2, we find that there is a high correlation between the percent of mobile residues as measured by NMR (Fig. 3A), and the percentage of surface residues from the model, at least when we define the surface as the line B-B'. For example, the ^{2}H-NMR spectrum of [$^2H_5$]tryptophan-labeled bR displays the full rigid powder pattern breadth, since all eight tryptophan residues reside within the matrix, and only a very small amount of central component signal intensity (equivalent to about 0.3 Trp) is present. In sharp contrast, the spectrum of [β-$^2H_2$]serine-labeled bR contains a superposition of a large isotropic component (arising from the 46% of the residues in the surface region), and a slightly more intense rigid component (due to the 54% of residues in the matrix), as shown in Figs. 1 and 3. Note, however, that the good correlation is almost eliminated by going either +2 residues (A-A' line or −2 residues (C-C' line), as shown in Fig. 3B. As discussed elsewhere (Keniry et al., 1984b), we obtain best agreement between the NMR results and Engelman's latest model, but our errors on quantitating the central component preclude any definitive statements as to which model is most realistic at this time. It should be noted that the results in Fig. 1 were reproduced for Phe, Val, Trp and Thr, on at least two sample preparations. Also, the sharp components all disappeared below ~−25°C, and on sample lyophilization, and are thus unlikely to be due to instrumental or other artifacts. The ^{2}H-NMR results are also quite consistent with our ^{13}C, ^{15}N and ^{19}F results, as discussed below. Using a different sample preparation technique, R.G. Griffin at the Massachusetts Institute of Technology has not observed the sharp ^{2}H (or ^{13}C) resonance that we have (private communication). We have no explanation for these differences, at this time. However,

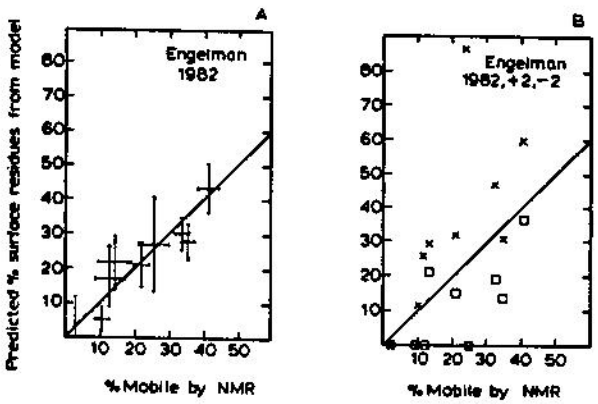

Fig. 3. Correlation between percent isotropic component in the ^{2}H-NMR spectrum and percent surface residues (A) in model of Fig. 2 using the line B-B' as the surface. (B) With surface definition lines A-A' (+ 2 residues, □) and C-C' (− 2 residues, x).

Haran and Lapidot (private communication to H.S.G.) have obtained sharp ^{15}N resonances from their preparation, and have reached identical conclusions as to surface mobility that we have, and similar results have been obtained by B.A. Wallace (private communication) using ^{1}H-NMR at high-field.

These results are all encouraging, since they imply that NMR has the *potential* to differentiate between different folding patterns for a 'solid' membrane protein. They are also surprising since they imply that 'isotropic' spectra may be obtained from at least some of the connecting loops, which we suggest have mobile structures. Further support for these ideas comes from recent work by Opella and coworkers (Frey et al., 1983), who have carried out somewhat similar investigations on the fd-phage coat protein dissolved in DMPC bilayers. They find a pronounced gradient of motion along the polypeptide chain, with residues close to the bilayer surface giving rise to narrow, 'isotropic' ^{2}H-NMR signals. What is even more surprising, they have suggested that mobile sidechain ^{2}H-NMR spectra may be observed (near the membrane surface), even when the NMR spectra of peptide-backbone (^{13}C, ^{15}N) labeled species indicate a lack of any substantial motion. The suggestion is that large amplitude motions about C^{α}-C^{β} and C^{β}-C^{γ} of, for example, phenylalanine residues, may be permitted near the membrane surface, giving rise to broad backbone label (C^{0},C^{α}) spectra, but to narrow spectra from sidechain-labeled species. Clearly, such observations may complicate quantitative determinations of folding patterns, although in the case of bR, we have obtained quantitative results consistent with Fig. 3A using [α-$^{2}H_{1}$]valine, a backbone-labeled species. Nevertheless, these results do suggest the need for further studies of bR folding patterns, and dynamics, using additional NMR methods, which probe both mainchain *and* sidechain dynamics. In addition, it will be most desirable to resolve and assign individual sites in this membrane protein.

We now discuss our progress in obtaining true 'high-resolution' NMR spectra of bR. First, we show in Fig. 4A–C solution state ^{13}C-NMR spectra (at 125.7 MHz) of leucine, bR and [$^{13}C^{0}$]Leu-bR, and in Fig. 4D–F we show the corresponding spectra taken under solid-state cross-polarization 'magic-angle' sample-spinning (CP-MASS) condition. Spectra of [$^{13}C^{0}$]Leu-bR show either an intense singlet (from surface residues, Fig. 4C), or a series of spinning-sidebands (from the matrix residues, Fig. 4F), while the natural-abundance spectra show broader and weaker signals in about the same region, which arise from C^{0} of *all* of the amino acids present in bR.

Under solid-state conditions, we selectively enhance the solid-like matrix amino acids, which are expected to have a chemical shift anisotropy (CSA) of ~200 ppm. It is of interest that it is possible to spin bR, a gelatinous material (up to ~2.5 kHz), without resorting to lyophilization. This permits observation of bR in its native state. Analysis of the spinning-sideband intensities as a function of spinning speed yields, from a Herzfeld-Berger calculation (Herzfeld and Berger, 1980), the principal components of the chemical shift tensor: $\sigma_{11} = 245 \pm 7$ ppm,

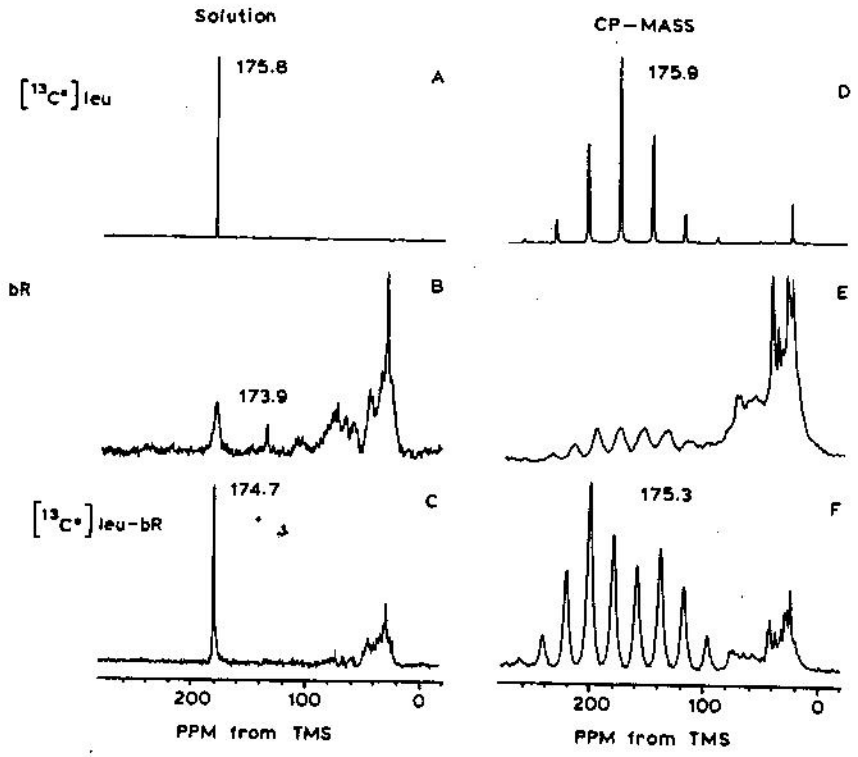

Fig. 4. Carbon-13 NMR spectra of [$^{13}C^0$]leucine, bacteriorhodopsin, and [$^{13}C^0$]Leu-bR, under solution and solid-state conditions. A, Solution spectrum of [$^{13}C^0$]leucine. B. Spectrum of unlabeled bR, under solution conditions. C, Spectrum of [$^{13}C^0$]Leu-bR, under solution conditions. D, CP-MASS spectrum of [$^{13}C^0$]leucine crystals. E, CP-MASS spectrum of unlabeled bR. F, CP-MASS spectrum of [$^{13}C^0$]Leu-bR. All spectra were recorded at 125.7 MHz (corresponding to a magnetic field strength of 11.7 Tesla). Solution conditions indicate single, 90° pulse excitation and ~2 watts WALTZ-16 ^{1}H decoupling. The CP mix times were all 1 ms. Chemical shifts are in ppm from an external sample of tetramethylsilane (TMS).

σ_{22} = 193 ± 7 ppm, and σ_{33} = 88 ± 7 ppm. These values are in good agreement with those obtained by R.G. Griffin and co-workers on [$^{13}C^0$]Leu-bR: σ_{11}=246 ppm, σ_{22}=191 ppm, σ_{33}=93 ppm (R.G. Griffin, private communication), and imply a rigid polypeptide backbone.

In principle, the chemical shifts observed should give information on the (primary and) secondary structure in the region of C^0 of leucine. There are discussions in the literature where it has been suggested that certain segments of bR are in β-sheet conformation and not in the α-helical form as generally envisaged (Jap et al., 1983), and it has been shown by others that ^{13}C-NMR chemical shifts are sensitive to these two possible conformational states. In particular, in poly(L-leucine), C^0 chemical shift differences of 3–6 ppm, have been noticed for different

secondary structures (Kricheldorf and Müller, 1983; Stulz et al., 1983). However, the linewidths in the MASS NMR spectra are about 500 Hz (4 ppm), so it is not possible to unequivocally rule out the presence of β-sheet in bR on the basis of the isotropic chemical shifts alone, although the results of Fig. 4F do indicate quite Lorentzian peaks having $\sigma_i = 175.3$ ppm, close to the ~175.8 ppm value expected for α-helical segments. Also, Griffin and co-workers (R.G. Griffin, private communication) using a DMPC-[C^0]Leu-bR system in which the bR undergoes fast axial rotation, have found two structures whose predicted lineshapes agree with the experimentally observed lineshape, one of which consists completely of α_I-helices tilted at an angle of ~20° with respect to the membrane normal.

Further work aimed at quantitating the $^{13}C^0$-NMR results of Fig. 4 (T_1,T_2, NOE, CP-mix time behavior, gas-chromatography/mass spectrometry of [$^{13}C^0$]Leu *N*-trifluoroacetyl methyl esters) are underway, and have the potential for very accurately determining the numbers of mobile/immobile residues in bR.

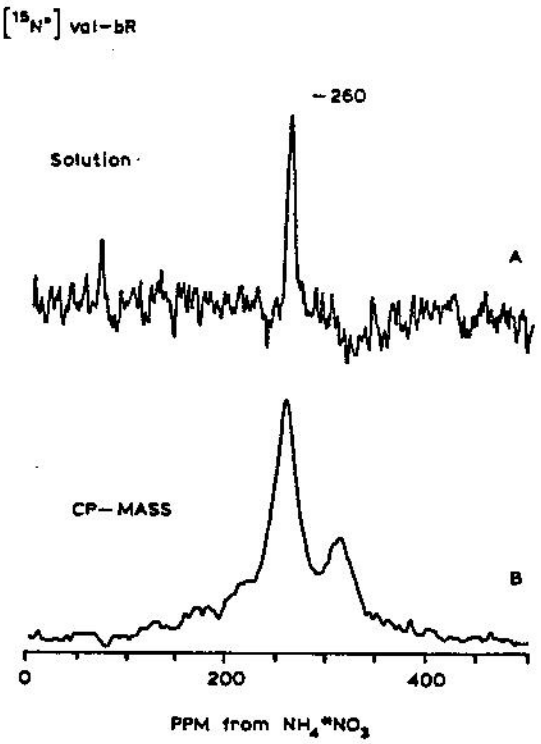

Fig. 5. Nitrogen-15 NMR spectra of [$^{15}N^0$]Val-bR under solution and solid-state conditions at 50.7 MHz (corresponding to a magnetic field strength of 11.7 Tesla). A, Spectrum under solution conditions, 30 μs pulse excitation, 36 000 scans, recycle time of 2 s, ~2 watts WALTZ-16 ^{1}H decoupling. B, CP-MASS spectrum, 6 μs 90° pulse width, 42 000 scans, 1.5 s recycle time, 1 ms mix time, and a spinning speed of 2.5 kHz. Chemical shifts are in ppm from an external sample of 1 M $NH_4{}^{15}NO_3$.

We have also performed similar preliminary NMR experiments on ^{15}N-labeled bR. Nitrogen-15, while not a very attractive nucleus for NMR spectroscopy due to its low gyromagnetic ratio and low natural abundance, nonetheless has the advantage that natural abundance (0.37%) background signals will be even lower than with ^{13}C. Fig. 5 shows the ^{15}N solution, and CP-MASS spectra of [$^{15}N^0$]Val-bR. Again, we notice the presence of a narrow signal in the solution spectrum (Fig. 5A) and the presence of rigid, crystalline residues (inside the surface) in the CP-MASS spectrum (Fig. 5B). The linewidths in the MASS spectrum are ~1000 Hz (20 ppm), so as with ^{13}C, we are unable at present to answer the question as to the presence of β-sheet regions, as the shift difference between α-helical and β-sheet peptide bonds is only ~10 ppm (Förster et al., 1983).

In none of the ^{13}C or ^{15}N bR samples we have investigated to date have we seen resolved, single-residue peaks in the surface region. Resolving individual surface amino acids in a native membrane protein with NMR would, however, be of exceptional interest, since we could thereby pinpoint with much better

TABLE 1
Comparison between ^2H-NMR data on labeled bR and the predictions of model-building[a]

Amino acid	Number of residues[b]	% Surface residues		% Surface residues after trypsin		
		NMR[c]	Model[a]	NMR	−10[d]	−21[d]
Glycine	25	32 ± 2	32	4	26	23
Valine	21	35 ± 2	29	7	29	29
Leucine	36	10 ± 2	6	3	6	6
Isoleucine	15	15 ± 4	13	–[e]	13	7
Serine	13	41 ± 4	46	18	36	36
Threonine	18	21 ± 3	22	2	18	18
Lysine	7	25 ± 4	29	–[e]	29	29
Arginine	7	25 ± 4	29	–[e]	29	29
Phenylalanine	13	11 ± 4[f]	23	3	23	17
Tyrosine	11	9 ± 4[f]	18	1	18	18
Tryptophan	8	2 ± 1.5	0	0	0	0

[a] The model of Engelman et al. (1982) was used to estimate surface versus non-surface residues, using line B-B' (Fig. 2) as the interface.

[b] Membranes were labeled with the appropriate deuterated amino-acids as described in Keniry et al., 1984b, the number of such residues are indicated.

[c] The integrated intensity of the central component, after correcting, as appropriate, for non-uniform isotope labeling in the precursor amino acid, breakdown, the estimanted residual HO^2H levels, and assuming a uniform incorporation into surface and non-surface regions.

[d] After trypsin cleavage to remove the number of C-terminal residues indicated.

[e] Not measured.

[f] At 37°C; other data at 4°C. After correction for distortions due to quadrupolar echo artefacts.

accuracy the number of surface residues (or at least, mobile residues) of a given type. ^{19}F-NMR appears to have considerable potential for this. ^{19}F has a spin I value of 1/2, so the spectra are not complicated by quadrupolar interactions, as found with ^{2}H. Fluorine is 100% naturally abundant and has a very high sensitivity (83% that of protons), and there are no naturally occurring residues containing ^{19}F in bR to contribute to a natural abundance background. Fluorine also has an extremely wide chemical shift range, and the chemical shift is highly sensitive to the environment (Sykes and Hull, 1978). With these points in mind, we have made bR labeled with *meta*-fluorophenylalanine ([*m*-^{19}F]Phe), and our ^{19}F-NMR results, obtained under solution conditions, appear quite exciting. As seen in Table 1, there are three Phe residues in the surface region of bR (using the Engelman model and the B-B′ surface line). The ^{19}F-NMR spectrum of [*m*-^{19}F]Phe-bR at 470 MHz shown in Fig. 6 strongly suggests a three component spectrum with chemical shifts of −111.9, −112.1 and −112.6 ppm (from $CFCl_3$). Although these results are very preliminary, the ability to resolve individual sites,

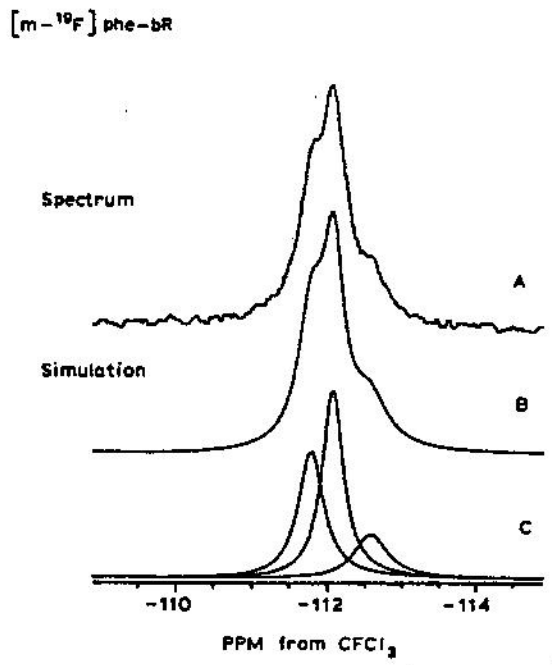

Fig. 6. ^{19}F-NMR spectrum of [*m*-^{19}F]Phe-bR, together with its computer simulations, at 470.4 MHz (corresponding to a magnetic field strength of 11.7 Tesla). A, Experimental ^{19}F-NMR spectrum, 25 μs pulse excitation, 44 000 scans, 0.34 s recycle time, coupled spectrum. B, Computer simulation of A using the three components indicated in C, which probably correspond to the three surface phenylalanine residues. The relative T_1-values have not yet been measured. Chemical shifts are in ppm from an external sample of $CFCl_3$.

and eventually to make assignments based on relaxation studies, chemical modification, pH titration, broadening by paramagnetic species, etc. (Tsetlin et al., 1984), should permit a much more detailed study of membrane proteins than has been possible to date.

III. Cleavage and aggregation

Proteolytic cleavage provides a chemical tool to modify bR, and can be conveniently used to verify the deductions made from the NMR studies on intact bR. If our ideas about the membrane surface are correct, it is reasonable to assume that a change in the number of mobile surface residues should change the solution-like signals. As a check of the surface picture provided by NMR, we have performed experiments on bR that was either enzymatically cleaved or crosslinked (using a carbodiimide). It has been reported that when bR is treated with trypsin, a small number of residues (10 or 21) are cleaved from the C-terminus (Wallace and Henderson, 1982). In our hands, amino acid analysis of a valine-labeled sample revealed that we had removed the 10 C-terminal residues. If this is general for all samples examined, then 2/25 glycines, 4/29 alanines, 0/21 valines, 0/36 leucines, 2/13 serines, 1/18 threonines, 0/13 phenylalanines, 0/11 tyrosines and 0/8 tryptophans would be removed in our trypsin digestion procedure. The effects of cleavage of the C-terminal fragment on our ^{2}H- and ^{13}C-NMR spectra are, however, far more dramatic than would be anticipated for removal of just 10 (or even 21) residues, as shown in Fig. 7 and Table 1.

For example, in the case of [γ-$^2H_6$]valine-bR (Table 1), the central component contributes 35% to the intensity of the native membrane spectrum, but only 7% of the intensity of the spectrum of the membrane (at 4°C) after digestion, even though as seen in Table 1, no valines are removed! Raising the temperature to 37°C does not change the contribution of the central component appreciably. Similarly, the intensity of the central component is decreased far more than anticipated for all other cleaved samples we have investigated, as shown in Fig. 7 and Table 1, and raising the sample temperature to 37°C again does not appreciably change the relative intensities of the two components. Consider for example the spectrum of [β,γ-$^2H_4$]threonine-labelled bR (Fig. 7D). At 4°C the intensity of the central component is 21 ± 3%, as shown in Table 1. This value compares well with the 22% surface threonines calculated on the basis of the model given in Fig. 2, since there are four surface threonines out of a total of 18 (4/18 = 22%). Cleavage of 10 (or 21) residues removes one threonine leaving only 18% in the surface (3/17 = 18%). However, experimentally we observe only a 2% central-component intensity (Fig. 7E,F and Table 1). While unexpected, we believe these results may be readily explained as being due to extensive aggregation of trypsinized purple membrane sheets. Even if in some samples we had actually removed all 21 C-

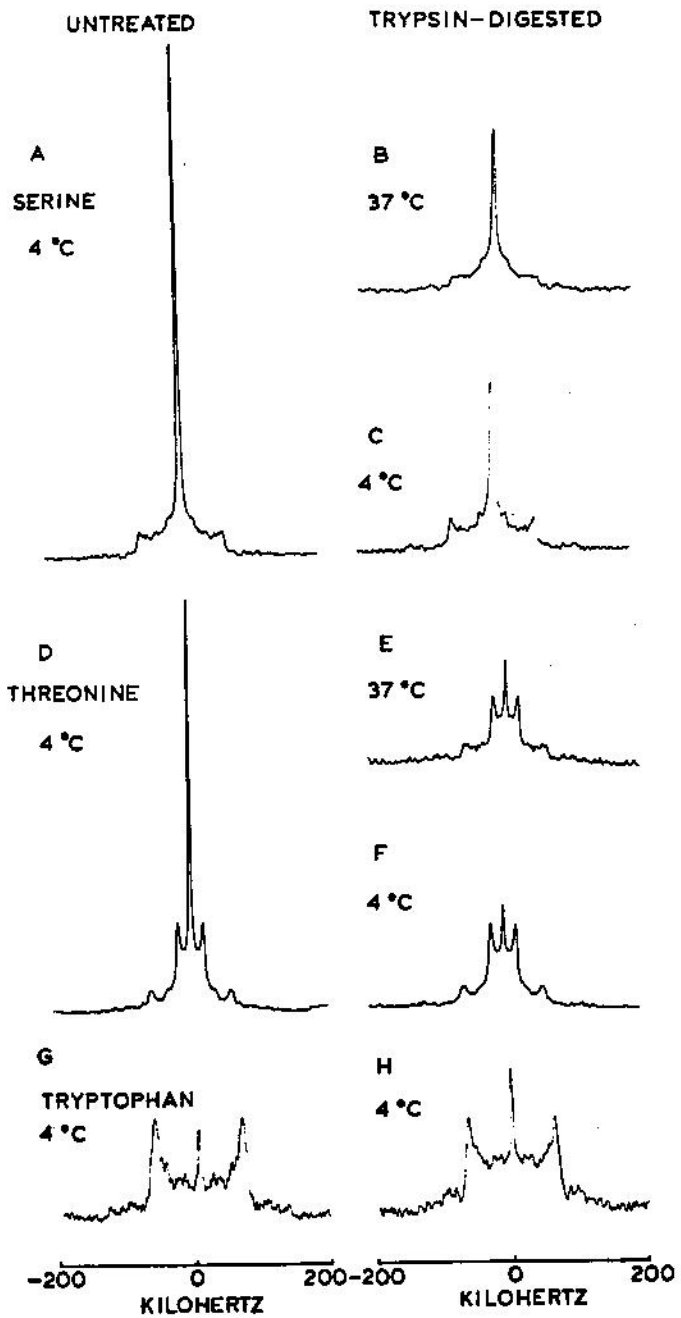

Fig. 7. Experimental deuterium NMR spectra showing the effect of tryptic cleavage of the C-terminus of bR. A, [β-$^2H_2$]Ser-bR at 4°C. B, Trypsin-digested [β-$^2H_2$]Ser-bR at 37°C. C, as B but at 4°C. D, [β,γ-$^2H_4$]Thr-bR at 4°C. E, Trypsin-digested [β,γ-$^2H_4$]Thr-bR at 37°C. F, as E but at 4°C. G, [ring-$^2H_5$]Trp-bR at 4°C. H, Trypsin-digested [ring-$^2H_5$]Trp-bR at 4°C. All spectra were recorded using the quadrupole-echo sequence at 55.3 MHz (corresponding to a magnetic field strength of 8.45 Tesla).

terminal residues, or if further proteolysis occurred during data acquisition, there is still essentially no relationship between the results observed and those expected on the basis of such a fragment removal, and proteolysis in magneto should generate peptides which would give rise to an extra *narrow* resonance.

Spin-lattice relaxation times (T_1) have been measured for the deuterated methyl-groups of valine-, leucine- and threonine-labeled purple membranes which have been treated with trypsin, and in all cases the T_1 values are, within experimental error, the same as for the native purple membranes, over a wide temperature range. This implies that the trypsin treatment only affects the surface residues, which are associated with the isotropic component, and not the residues giving rise to the solid-state powder pattern lineshape from the interior of the bilayer. Thus, our results strongly suggest that aggregation occurs upon trypsin treatment, and this causes an immobilization of all surface residues so that in the ^{2}H-NMR experiment, they become motionally indistinguishable from the rigid matrix residues. This notion receives additional support from the results of ^{13}C-NMR experiments, as discussed below.

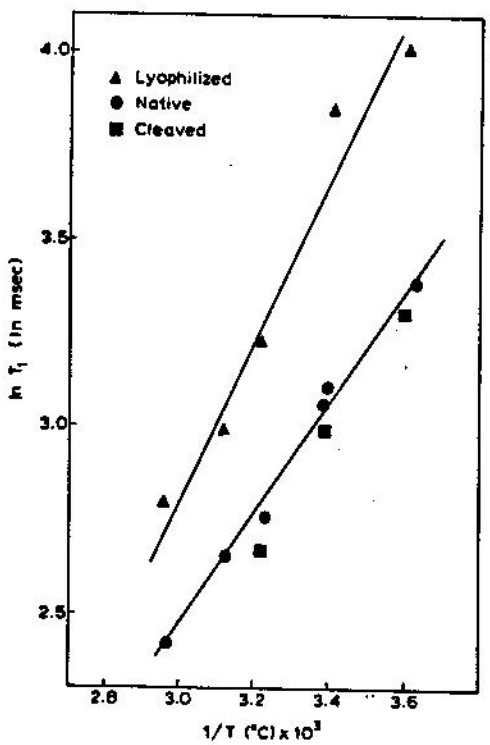

Fig. 8. Plots of lnT_1 for [*o*,*m*-$^2H_4$]Phe-bR as a function of temperature, for native (●), trypsin-cleaved (■) and lyophilized (▲) samples. Spectra were recorded at 55.3 MHz using a 180_x–τ–90_x–τ–90_y-echo sequence.

We now discuss the effects of other processes which should greatly alter surface interactions, including the effects of H_2O removal (by lyophilization), and of chemical cross-linking. In particular, we discuss the effects of lyophilization on the high-frequency motions of phenylalanine, which govern its spin-lattice relaxation behavior.

Figure 8 shows an Arrhenius plot of T_1 variation with temperature, for [$^2H_4$]phenylalanine-labeled purple membrane in the native state, lyophilized, and after trypsin treatment. As shown in Fig. 8, native and enzymatically-cleaved purple membranes both show very similar relaxation behavior, and the corresponding NMR spectra are all also quite similar, as shown in Fig. 9. The T_1 behavior of the lyophilized [$^2H_4$]Phe-bR sample, however, is rather different. The ^{2}H-NMR spectrum is similar to native bR, but the T_1 values are much longer, indicating less efficient relaxation, and the activation energy has increased from 12.8 kJ mol^{-1} to 17.9 kJ mol^{-1}. This shows that for the very hydrophobic phenylalanine sidechain, the interior of the membrane is influenced by the presence of water in the system. These results clearly indicate that caution needs to be exercised in the interpretation of NMR spectra obtained on lyophilized samples, since the dynamic nature of the membrane is, perhaps not surprisingly for a protein, greatly influenced by the presence of water. Indeed, even the drastic effects of aggregation, and of chemical crosslinking (Figs. 8 and 9B,C) do not have as large an effect on the ^{2}H-NMR lineshape or T_1 as does dehydration of the membrane.

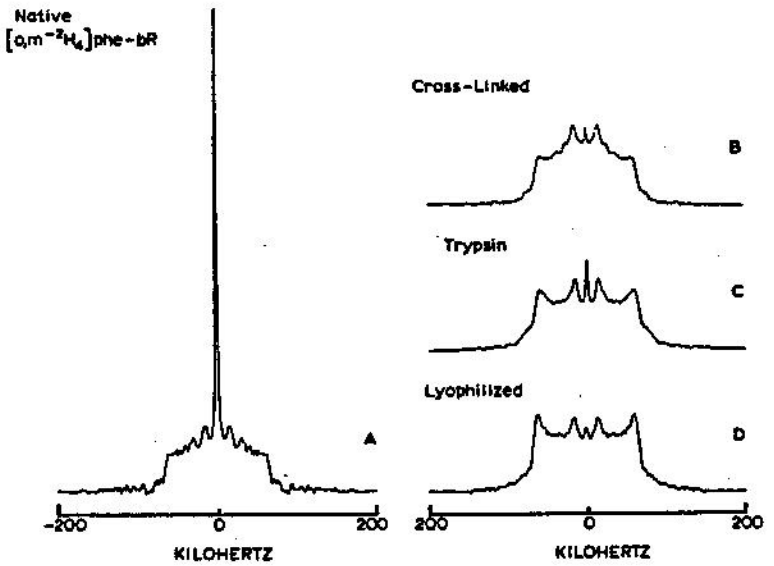

Fig. 9. Deuterium NMR spectra of [$^2H_4$]Phe-bR subjected to various treatments, at 55.3 MHz. A, Native. B, Crosslinked with dicyclohexylcarbodiimide. C. Trypsin-cleaved. D, Lyophilized.

Using the model of small angle librations for T_1-relaxation in [$^2H_4$]Phe-bR and [phenyl-d_4]poly(butylene terphthalate) (Lewis et al., 1984; Cholli et al., 1984), our results imply that hydration of the protein interior causes a general lowering of the barriers to rotation of the aromatic phenyl ring in phenylalanine, and similar effects may well be observed, or even accentuated, for tyrosine and tryptophan.

The effects of cleavage/aggregation we have discussed above are also supported by ^{13}C-NMR, where the same trend is seen when one compares native and cleaved solution spectra of [ring-$^{13}C_6$]phenylalanine-labeled bR, as shown in Fig. 10. Upon cleavage, the isotropic peak undergoes a marked reduction in intensity relative to the natural abundance membrane background signal, indicating, we believe, extensive aggregation and a general 'solidification' of the membrane surface. However, this result must be regarded as preliminary since we have not yet measured T_1/NOE values of cleaved and native samples. Nevertheless, something dramatic must occur upon trypsinization/aggregation.

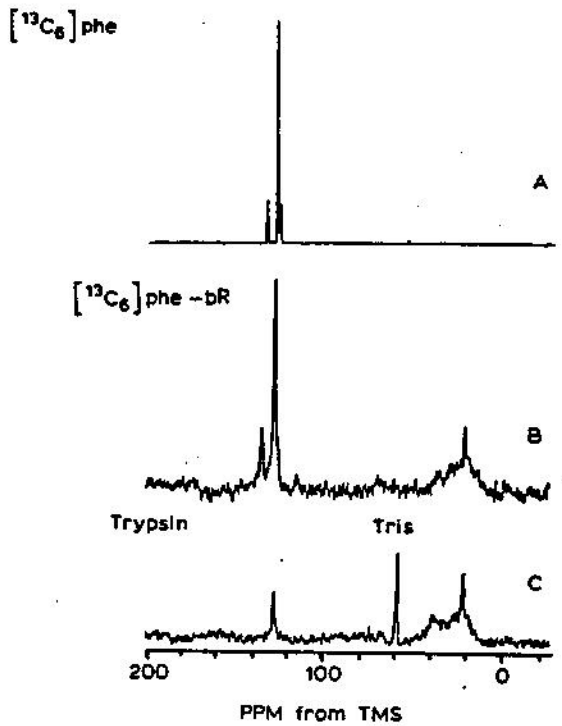

Fig. 10. Proton-decoupled 125.7 MHz carbon-13 NMR spectra of [ring-$^{13}C_6$]Phe, [$^{13}C_6$]Phe-bR and trypsin-cleaved [$^{13}C_6$]Phe-bR, recorded under solution-NMR conditions consisting of single, 25 μs, −90° pulse excitation and ~2 watts of WALTZ-16 ^{1}H decoupling. A, [$^{13}C_6$]Phe in solution. B, [$^{13}C_6$]Phe-bR, native sample. C, as B but after trypsin-cleavage of the C-terminus (and aggregation). The peak labeled Tris around 60 ppm is due to Tris (tris(hydroxymethyl)aminomethane).

We have also obtained sodium dodecylsulfate (SDS) polyacrylamide electrophoresis gels for native, trypsin cleaved and chemically crosslinked purple membranes. The results indicate that the trypsin treatment removes only a few amino acid residues, and does not cause chemical aggregation, while the crosslinked sample is of very high molecular weight, and suggests that there are at least three bR molecules per crosslinked unit.

Taken together, these results all strongly suggest to us that very dramatic changes in surface dynamics occur on removing the C-terminal fragment of bR, or upon crosslinking. Specifically, our results imply that the membrane aggregation phenomenon known to accompany proteolysis causes an immobilization of virtually all surface residues during surface-contact.

IV. Future potential

Our results thus indicate that NMR spectra may be very sensitive to the state of aggregation of biological membranes. Such a spectroscopic probe of surface structure could have considerable potential for studying the nature of cell-cell contacts in more complex systems, such as mammalian cells in tissue culture or, for example, the thrombin-catalyzed aggregation of blood platelets, where the effects of a variety of substances which modulate cell-cell interaction could be investigated, at the molecular level, using a non-perturbing spectroscopic probe.

Acknowledgements

We would like to thank Professors T. Ebrey and W. Stoeckenius for their kind gifts of *Halobacterium halobium*, and Catherine Flynn for help in sample preparation. We also thank Drs. R.G. Griffin and L. Lapidot for providing copies of manuscripts prior to publication.

This work was supported in part by the U.S. National Institutes of Health (grant HL-19481) and the U.S. National Science Foundation (grants PCM 83-02512 and 84-16771).

A.C.K. is on leave from the Raman Research Institute, Bangalore 560 080, India.

X.S. was supported by The Peoples' Republic of China, Chemistry Graduate Program, 1983–1984.

E.O. is a United States Public Health Service Research Career Development Awardee, 1979–1984 (grant CA-00595).

References

Agard, D.A. and Stroud, R.M. (1982) Linking regions between helices in bacteriorhodopsin revealed. Biophys. J. 37, 589–602.

Cholli, A.L., Dumais, J.J., Engel, A.K. and Jelinski, L.W. (1984) Aromatic ring flips in a semicrystalline polymer. Macromolecules 17, 2399–2404.

Engelman, D.M. and Zaccai, G. (1980) Bacteriorhodopsin is an inside-out protein. Proc. Natl. Acad. Sci. USA 77, 5894–5898.

Engelman, D.M., Goldman, A. and Steitz, T.A. (1982) The identification of helical segments in the polypeptide chain of bacteriorhodopsin. In: *Methods in Enzymology*, Vol. 88, Chapter 11, pp. 81–88. Editor: L. Packer, Academic Press, New York.

Förster, H.G., Müller, D. and Kricheldorf, H.R. (1983) Secondary structures of peptides: 5. ^{15}N n.m.r. CP/MAS spectroscopy of solid polypeptides and gramicidin-S. Int. J. Biol. Macromol. 5, 101–105.

Frey, M.H., Hexem, J.G., Leo, G.C., Tsang, P., Opella, S.J., Rockwell, A.L. and Gierasch, L.M. (1983) Solid-state NMR of peptides in membrane bilayers. In: *Proc. 8th Am. Pept. Symp.*, pp. 763–771. Editors: V. Hruby and D.H. Rich, Pierce Chem. Co., Rockford, Il.

Henderson, R. and Unwin, P.N.T. (1975) Three dimensional model of purple membrane obtained by electron microscopy. Nature 257, 28–32.

Herzfeld, J. and Berger, A.E. (1980) Sideband intensities in NMR spectra of samples spinning at the magic angle. J. Chem. Phys. 73, 6021–6030.

Jap, B.K., Maestre, M.F., Hayward, S.B. and Glaeser, R.M. (1983) Peptide-chain secondary structure of bacteriorhodopsin. Biophys. J. 43, 81–89.

Keniry, M.A., Kintanar, A., Smith, R.L., Gutowsky, H.S. and Oldfield, E. (1984a) Nuclear magnetic resonance studies of amino acids and proteins. Deuterium nuclear magnetic resonance relaxation of deuteriomethyl-labeled amino acids in crystals and in *Halobacterium halobium* and *Escherichia coli* cell membranes. Biochemistry 23, 288–298.

Keniry, M.A., Gutowsky, H.S. and Oldfield, E. (1984b) Surface dynamics of the integral membrane protein bacteriorhodopsin. Nature 307, 383–386.

Khorana, H.G., Gerber, G.E., Herlihy, W.C., Gray, C.P., Anderegg, R.J., Nihei, K. and Bieman, K. (1979) Amino acid sequence of bacteriorhodopsin. Proc. Natl. Acad. Sci. USA 76, 5046–5050.

Kinsey, R.A., Kintanar, A., Tsai, M.D., Smith, R.L., Janes, N. and Oldfield, E. (1981) First observation of amino acid side chain dynamics in membrane proteins using high field deuterium nuclear magnetic resonance spectroscopy. J. Biol. Chem. 256, 4146–4149.

Kricheldorf, H.R. and Müller, D. (1983) Secondary structure of peptides, 3. ^{13}C NMR cross polarization/magic angle spinning spectroscopic characterization of solid polypeptides. Macromolecules 16, 615–623.

Lewis, B.A., Rice, D.M., Olejniczak, E.T., Das Gupta, S.K., Herzfeld, J. and Griffin, R.G. (1984) Deuterium NMR studies of molecular dynamics in bacteriorhodopsin: Analysis of lineshapes and intensities for phenylalanine, tyrosine, and leucine sidechains. Biophys. J. 45, 213a.

Oldfield, E. and Chapman, D. (1972) Dynamics of lipids in membranes: Heterogeneity and the role of cholesterol. FEBS Lett. 23, 285–297.

Oldfield, E., Chapman, D. and Derbyshire, W. (1971) Deutron resonance: A novel approach to the study of hydrocarbon chain mobility in membrane systems. FEBS Lett. 16, 102–104.

Ovchinnikov, Y.A. (1982) Rhodopsin and bacteriorhodopsin: Structure-function relationship. FEBS Lett. 148, 179–191.

Ovchinnikov, Y.A., Abdulaev, N.G., Feigina, M.Y., Kiselev, A.V., Lobanov, N.A. and Nasimov, I.V. (1978) Primary structure of bacteriorhodopsin. Bioorg. Khim. 4, 979–981.

Ovchinnikov, Y.A., Abdulaev, N.G., Feigina, M.Y., Kiselev, A.V. and Lobanov, N.A. (1979) The structural basis of the functioning of bacteriorhodopsin: An overview. FEBS Lett, 100, 219–224.

Seelig, J. (1977) Deuterium magnetic resonance: theory and application to lipid membranes. Q. Rev. Biophys. 10, 353–418.

Smith, R.L. and Oldfield, E. (1984) Dynamic structure of membranes by deuterium NMR. Science 225, 280–288.

Stulz, J., Müller, D., Hull, W.E. and Kricheldorf, H.R. (1983) FT-IR and ^{13}C NMR CP/MAS study on tacticity and secondary structure of poly(D,L-leucine)s. Makromol. Chem. 184, 1311–1322.

Sykes, B.D. and Hull, W.E. (1978) Fluorine nuclear magnetic resonance studies of proteins. In: *Methods in Enzymology*, Vol. 49, Chapter 13. pp. 270–295. Editors: C.H.W. Hirs and S.N. Timasheff. Academic Press, New York.

Tsetlin, V.I., Zakis, V.I., Ovechkina, G.V., Kuryatov, A.B., Balashova, T.A., Arseniev, A.S., Maiorov, V.N. and Ivanov, V.T. (1984) Preparation, ^{19}F NMR and EPR studies of fluorine-containing and spin-labeled bacteriorhodopsin derivatives. Biol. Memb. 1, 838–857.

Wallace, B.A. and Henderson, R. (1982) Location of the carboxyl terminus of bacteriorhodopsin in purple membrane. Biophys. J. 39, 233–239.

Wagner, G. and Wüthrich, K. (1982) Sequential resonance assignments in protein ^1H nuclear magnetic resonance spectra. Basic pancreatic trypsin inhibitor. J. Mol. Biol. 155, 347–366.